Available online at www.sciencedirect.com
SCIENCE DIRECT®
Journal of Catalysis 221 (2004) 32–42
JOURNAL OF CATALYSIS
www.elsevier.com/locate/jcat

An emergent catalytic material: Pt/ZnO catalyst for selective hydrogenation of crotonaldehyde

F. Ammari,[a] J. Lamotte,[b] and R. Touroude [a,*]

[a] *LMSPC, UMR 7515 du CNRS, ECPM, ULP, 25 rue Becquerel, 67087 Strasbourg cedex 2, France*
[b] *ISMRA, UMR 6506 du CNRS, Catalyse et Spectrochimie, 6 bd du Maréchal Juin, 14050 Caen, France*

Received 17 April 2003; revised 20 June 2003; accepted 20 June 2003

Abstract

By using modifiers in platinum catalysts it is possible to modulate the hydrogenation selectivity in α,β-unsaturated aldehydes carbonyl bond with regard to olefinic bond hydrogenation. The challenge is to find an emergent catalytic material able to produce 100% unsaturated alcohol. In this field, 1% Pt/ZnO catalysts were tested in hydrogenation of crotonaldehyde, in gas phase, at atmospheric pressure. The catalysts were prepared by impregnation of ZnO from two different precursors, H_2PtCl_6 and $Pt(NH_3)_4(NO_3)_2$, followed by calcination at 673 K and tested after reduction at different temperatures, 473–773 K. The ex-nitrate and ex-chloride catalysts showed quite different catalytic behaviors. The ex-chloride was much more active and selective; in certain conditions 90% crotyl alcohol selectivity was reached. Different techniques (TPR, XRD, TEM, XPS, FTIR) were used to characterize both types of catalysts and to correlate the structure and the reactivity. The Lewis acidity of ZnO after the reduction treatment and the formation of PtZn alloy were found to be the key factors leading to high crotyl alcohol yield. It was proposed that modification of the electronic properties of platinum both by alloying to zinc and by Lewis acidity of the support reinforced by chlorine changes the adsorption mode of crotonaldehyde by favoring the binding of the terminal oxygen of the molecule to the electronically modified platinum atom.

Keywords: Crotonaldehyde selective hydrogenation; Pt/ZnO catalysts; Chlorine content effects; PtZn alloy; Lewis acidity of ZnO

1. Introduction

An emergent material in heterogeneous catalysis is, for example, a material able to catalyze a reaction which is usually performed by a noncatalytic process. The heterogeneous catalytic process is always easier to handle than any other process and leads to a lower amount of waste products with lower risk for the environment. For example, in the past few years considerable effort has been devoted to develop a heterogeneous catalytic system able to perform selective hydrogenation of the carbonyl function of α,β-unsaturated aldehydes into unsaturated alcohols with a high yield. This process could replace the metal hydrides usually used in preparative organic chemistry for this purpose [1,2]. The production of unsaturated alcohol from α,β-unsaturated aldehydes is a very important reaction in the preparation of many pharmaceutical, agrochemical, and fragrance compounds.

Hydrogenation reactions are mostly carried out with supported group VIII metal catalysts. Thermodynamically the hydrogenation of the carbonyl group into an unsaturated aldehyde is not favored. To achieve a high selectivity, this thermodynamic constraint must be removed by a preferential adsorption of the carbonyl function on the catalyst surface. It was found that the addition of promoters [1–3] and the use of bimetallic catalysts [4,5] improve largely the selectivity in unsaturated alcohols of platinum-based catalysts. The improvement of selectivity in a bimetallic catalyst was attributed to the possible existence of polar sites in the bimetallic phase able to change the adsorption structure of the reactant. An alternative way to improve the selectivity of platinum was the use of a reducible support [6]. In this field the TiO_2-supported Pt catalysts have attracted much attention because of the increase in selectivity obtained after a high-temperature reduction treatment of the catalyst. The authors [6,7] interpreted this selectivity improvement by the creation of oxygen vacancies in the TiO_x phase which interact with the oxygen end of the C=O bond, polarize this bond, and then favor the intermediate which, after ad-

* Corresponding author.
E-mail addresses: jean.lamotte@ismra.fr (J. Lamotte), touroude@chimie.u-strasbg.fr (R. Touroude).

0021-9517/$ – see front matter
doi:10.1016/S0021-9517(03)00290-2

dition of hydrogen atoms, gives the crotyl alcohol product. In this line of research CeO_2 [8–11], SnO_2 [12], and ZnO [13] were also found to influence the selectivity of platinum catalysts. The presence of chlorine, brought by the metallic precursor, played a prominent role in this catalyst type. It affected the selectivity of crotonaldehyde hydrogenation into crotyl alcohol in a detrimental way on Pt/CeO_2 [10,11] and Pt/SnO_2 [12] and in a beneficial way on Pt/ZnO [13]. In the latter case a parallel was found between the evolution of the crotyl alcohol selectivity and the PtZn alloy formation. Therefore, it was proposed that the catalytic surface consisted of PtZn entities in which the bond polarization, increased by the vicinity of chlorine, forced the molecule to adsorb by the C=O polar bond. On the other hand, Boffa et al. [14] found that submonolayer quantities of metal oxides, such as AlO_x, TiO_x, VO_x, FeO_x, ZrO_x, NbO_x, TaO_x, and WO_x, deposited on Rh foils, enhanced the reactions involving the C–O bond hydrogenation. The enhancement in CO, CO_2, and acetone hydrogenation was attributed to the formation of a Lewis acid-base complex between the O end of the polar CO bond with exposed metal cations of the oxide located at the boundary between the oxide and the Rh [14].

In this research field and to understand better the remarkable effect of chlorine on the performance of Pt/ZnO which could be linked to the ZnO Lewis acidity we persevered by studying the crotonaldehyde hydrogenation on Pt supported on ZnO, choosing catalysts with 1% metal content. Our choice of this lower Pt content compared to the 5% Pt/ZnO studied in [13] was a compromise: high enough Pt content to measure the activities in our experimental conditions but low enough to perform Fourier-transformed infrared spectroscopy analysis of the catalysts. This analysis could give more information on the surface nature such as electronic properties of metals and the nature and the power of the support acidity. In fact, with 5% Pt supported on ZnO, no IR transparency could be detected, due to the high ZnO reduction; using 1% Pt-supported ZnO, we could expect a more dispersed metallic phase and a decrease in ZnO reduction and then an increase in IR transparency. On the other hand, it was also of a great interest to analyze the influence of the Pt content on the reaction behavior of a Pt/ZnO catalytic system which shows exceptional properties in selective crotonaldehyde hydrogenation. Moreover, to understand the differences in the catalytic behavior of the catalysts prepared from different metal precursors, beside FTIR characterization, the samples were characterized by other methods, in particular X-ray diffraction (XRD), photoelectron spectroscopy (XPS), and transmission electron microscopy (TEM) to control the alloy formation and the size of particles.

2. Experimental

2.1. Catalyst preparation

The 1 wt% Pt-supported catalysts were prepared by impregnation of ZnO (Asturienne des Mines, 42.6 m^2/g) with an aqueous solution of H_2PtCl_6 or $[Pt(NH_3)_4](NO_3)_2$ salts (Strem Chemicals), followed by evaporation of water and drying overnight at 393 K. The samples were calcined, 4 h, in air, at 673 K. Prior to the reaction studies, the samples were reduced, 4 h, at different temperatures. In the text, the catalysts are called ex-chloride and ex-nitrate catalysts, respectively.

2.2. Crotonaldehyde hydrogenation

The crotonadehyde hydrogenation was carried out in the gas phase at atmospheric pressure of hydrogen, usually at 353 K, using a quartz tube reactor. The crotonaldehyde (Fluka puriss) (100–300 µl) was introduced in a trap at 273 K, which maintained 8 Torr as crotonaldehyde partial pressure, with very few exceptions specified in the text. The quantity of catalyst used varied between 0.1 and 0.3 g. The reaction products, *trans* and *cis* crotyl alcohol (CROTOL), butanal (BAL), butanol (BOL), hydrocarbons (HC), and minor by-products (generally $< 1\%$) were analyzed by gas chromatography with a DB-Wax column (30 m long, 0.53 mm of inner diameter). The identification of the various hydrocarbons was occasionally made using a CP-SIL 5CB column. The minor by-products are taken into account in the calculation of the product selectivities but they were not reported in Tables 1–3 for the sake of clarity. The crotonaldehyde, used without further purification, contained 0.1–0.3% butanal, therefore the selectivity values were always compared at conversions higher than 4% to minimize the errors. In fact, at 4% crotonaldehyde conversion, the butanal selectivity error could reach a maximum 10%, at lower conversion it would be more.

2.3. Characterization

The catalysts and the support were characterized by atomic absorption spectroscopy (AAS), nitrogen adsorption (BET), X-ray photoelectron spectroscopy, temperature-programmed reduction (TPR), Fourier-transformed infrared spectroscopy (FTIR), and transmission electronic microscopy, after different pretreatments.

The quantities of chlorine and platinum were obtained by AAS at CNRS, Vernaison (France). BET surface areas and total pore volume were obtained using a Coulter SA3100 machine. The XRD analyses were performed on a Siemens D 5000 polycrystalline diffractometer using Cu-K_α radiation. The zincite phase could be identified in every spectrum. However, the spectra, reported here, are limited to the 38.5–42.5 2θ region, where Pt (111) (JCPS 4-0802) and Pt–Zn (111) (JCPS 6-0604), the most intense lines, are expected for Pt and PtZn phases, respectively. XPS measurements were carried out with a VG ESCA III spectrometer with a magnesium anode ($K_\alpha = 1253.6$ eV). Sample treatments were carried out in situ in the preparation chamber attached directly to the analysis chamber. The $Pt4f_{7/2}$ binding energy (BE),

Table 1
Crotonaldehyde hydrogenation on 1% Pt/ZnO, precursor $Pt(NO_3)_2(NH_3)_4$, reduced at different temperatures ($P_{crotal} = 8$ Torr, $P_{H_2} = 752$ Torr)

Reduction T (K)	473		573		673		773			
Reaction T (K)	353		353		353		353	393	413	
Number of cycles[a]	1		1		1		1			
F (μmol s^{-1})	0.23		0.23		0.15		0.14			
Time on stream (min)	12	72	12	72	12	72	8	18	30	111
C_v (%)	10.7	4.6	8.6	4.5	24.0	5.3	4.7	8.4	11.8	6.0
A (μmol s^{-1} g$_{Pt}^{-1}$)	12.0	5.2	9.9	5.2	17.7	3.9	3.3	5.9	8.3	4.2
Selectivity (%)										
HC	2.0	2.0	3.0	3.8	0.7	1.7	4.5	2.0	1.3	1.5
BAL	63.3	65.7	61.4	68.5	39.5	46.8	43.5	50.7	58.6	55.3
BOL	8.1	3.2	7.8	2.7	21.2	4.4	14.3	8.2	6.4	9.2
CROTOL	25.0	29.0	26.0	25.0	38.0	47.0	33.0	37.0	33.0	34.0
C=O/C=C		0.5		0.4		1.0	0.8	0.8	0.6	0.7
BAL yield	7.6	3.4	6.1	3.6	7.0	1.8	1.5	3.0	5.0	2.3
CROTOL yield (μmol s^{-1} g$_{Pt}^{-1}$)	1.0	1.5	2.6	1.3	6.7	1.9	1.1	2.2	2.6	1.4

[a] Cycle is equivalent of one reduction treatment followed by one experiment.

Table 2
Crotonaldehyde hydrogenation on 1% Pt/ZnO, precursor H_2PtCl_6, reduced at different temperatures ($P_{crotal} = 8$ Torr, $P_{H_2} = 752$ Torr)

Reduction T (K)	473				573				673				773			
Reaction T (K)	353				353				353				353			
Number of cycles	1		2	4	1		2		4		1		2		4		1	
F (μmol s^{-1})	0.16		0.38	0.14	0.17		0.41		0.27		0.21		0.35		0.18		0.2	
Time on stream (min)	12	88	82	78	12	82	12	84	12	76	12	82	12	82	12	84	12	74
C_v (%)	36.6	29	10.1	10	45.8	25.7	30.2	9	21.5	9.5	31.0	11.7	27	8.5	15.8	7.3	10	7.4
A (μmol s^{-1} g$_{Pt}^{-1}$)	19.8	16	13	5	26.3	14.7	41.4	12.4	19.8	8.7	22.4	8.4	31.9	10	9.3	4.3	6.2	4.6
Selectivity (%)																		
HC	3.7	0.8	2.4	0.4	9.1	0.7	7.1	1.2	0.9	0.1	3.3	0.8	1.1	0.7	3.5	0.7	0	0
BAL	44	34	24.6	40	29	18.7	18.4	14.2	17.1	12.6	15.9	12.9	13.9	13.5	11.3	8.4	12.9	14.2
BOL	6.4	5	2.7	2.8	8.1	4.6	4.9	2.8	2.3	1.7	5.2	1.8	3.4	1.6	3.2	0.7	2.9	0.8
CROTOL	45.6	60	69.8	56	53	76	74	83	79	85	73.4	83.1	81	83.2	80	89	84	85
C=O/C=C			2.7	1.4				5.0		6.1				5.6		9.9		5.7
BAL yield		5.4	3.2	2.0		2.7		1.8		1.1		1.1		1.4		0.4		0.7
CROTOL yield (μmol s^{-1} g$_{Pt}^{-1}$)		9.6	9.1	2.8		11.2		10.3		7.4		7		8.3		3.8		3.9

γ(4f) (half-width at half-maximum) and peak areas were deduced using a curve-fitting procedure described in Ref. [13]. The $Pt4f_{7/2}$ BE were referenced to the $Zn3p_{3/2}$ BE, 88.3 eV, recorded in the same spectra. O1s BE was found at 530.5 eV. The C1s was too small and not well defined enough to be taken as a BE reference. The reducibility of the catalysts was followed by TPR in a flow system with a 1.5% H_2/Ar using an X-sorb-(S) instrument (GIRA society). After in situ calcination at 673 K and cooling to room temperature, the samples were flushed by Ar and by a H_2/Ar mixture, and then the TPR was recorded with a linear ramp of temperature (8 K/min) from 293 to 873 K. The samples were kept at this temperature for 1 h. The calibration measurement of the apparatus was repeated at the end of each experiment and then the moles of hydrogen consumed were deduced from the peak area. TEM analyses were performed on a Topcon 002B electron microscope, operating at 200 kV, with a point-to-point resolution of 0.18 nm in HRTEM mode. Some catalyst grains, taken after the different catalytic pretreatments performed in the catalytic apparatus, were ground and diluted in an ethanolic solution. One drop of this solution, previously dispersed in an ultrasonic tank, was deposited onto a Cu grid coated by a holey carbon film and dried in air. Various regions of the grid were observed and the particle sizes were measured from the observation of 250 to 500 particles. The following formula was used to calculate the mean surface diameter, $d_s = \sum n_i d_i^3 / \sum n_i d_i^2$, where n_i is the number of particles of diameter d_i. Nanoprobe X-ray fluorescence was also used to check the nature of elements present in the selected area ($d = 14$ nm). The IR measurements were per-

Table 3
Crotonaldehyde hydrogenation, at different temperatures, on 1% Pt/ZnO ex-chloride, reduced at 673 K

Reaction T (K)	313	353	393
F (μmol s^{-1})	0.2	0.2	0.8
Conversion (%)	7.9	19.9	10.7
Activity (μmol s^{-1} g$_{Pt}^{-1}$)	5.5	13.8	29.3
Selectivity (%)			
HC	0.8	0.6	0.9
BAL	8.7	14.9	16.7
BOL	2.7	2.2	0.9
CROTOL	88.0	82	81
BAL yield (μmol s^{-1} g$_{Pt}^{-1}$)	0.5	2.0	4.9
CROTOL yield (μmol s^{-1} g$_{Pt}^{-1}$)	4.8	10.9	23.7
E_a of total action (kJ/mol^{-1})		21 ± 0.2	
E_a of CTOL formation (kJ/mol^{-1})		20 ± 1	
E_a of BAL formation (kJ/mol^{-1})		28 ± 3	

formed with an infrared quartz cell, where in situ treatments were carried out at the desired temperature. After evacuation at 473 K, pulses of CO or pyridine were introduced at room temperature. The spectra were recorded using a Nicolet Magna 550 spectrometer.

3. Results

3.1. Crotonaldehyde hydrogenation

No hydrogenation activity was observed on the support alone, after reduction at 673 K, for the crotonaldehyde hydrogenation performed at 353 K. We just remarked on the formation of a very low quantity of by-products ($< 0.5\%$) which were not identified.

In Tables 1 and 2 the conversions (C_v%), product selectivities (HC, BAL, BOL, CROTOL (%)), and activities (μmol s^{-1} g$_{Pt}^{-1}$), observed during the time on stream, in the initial period (at 12 min) and in the quasi-steady-state regime (more than 70 min), for the ex-nitrate and ex-chloride catalysts are reported, respectively. These catalysts were reduced at different temperatures, 473, 573, 673, and 773 K. For the ex-nitrate catalyst, the reactivity was studied in the first catalytic run, after one reduction treatment while, for the ex-chloride catalysts, successive catalytic cycles (cycle is reduction treatment followed by experiment at 353 K) were performed and the reactivity is reported in the first, second, and fourth catalytic runs. The BAL and CROTOL yields ($A * \mathrm{SBAL}$ and $A * \mathrm{SCROTOL}$, respectively) and the C=O/C=C hydrogenation ratios ((SCROTOL + SBOL)/(SBAL + SBOL)) were also calculated.

Both catalysts showed a deactivation period at the beginning of the time on stream in which the selectivities were not exactly the same as those obtained in the steady-state regime. However, the most striking features in the product distributions were already present in the initial as well as in the stable regime; namely, butanal was mostly produced on the ex-nitrate catalyst while, on the ex-chloride, crotyl alcohol prevailed. In addition to the main products, butanol and hydrocarbons were formed. Looking at the evolution of these minor products during the time on stream, one observes (i) on the ex-nitrate catalyst, butanol initially appeared in a significant amount and then decreased at the expense of butanal and crotyl alcohol while hydrocarbons remained at a constant low value (1–4%) all along the time on stream, (ii) on the ex-chloride catalyst which formed mainly crotyl alcohol, hydrocarbons appeared initially in large amounts to deeply decrease at the expense of crotyl alcohol; butanol followed the same evolution, in a less pronounced manner. Hydrocarbons, initially formed, contain only C4 products, butadiene, butenes, and butane, which are reasonably assumed to be formed by dehydration–hydrogenation reactions of crotyl alcohol; C3 hydrocarbons, which would indicate a decarbonylation reaction, were not observed. This result is interesting to compare with those found on Pt/SiO_2 [5,15,16] and Pt/TiO_2 reduced at low temperature [17] where the decarbonylation reaction was suggested to be the origin of the deactivation step.

A detailed deactivation kinetic modeling was not undertaken in the scope of this paper where we have rather focused our analysis on the data obtained in the steady-state regime, keeping in mind that the deactivation did not change significantly the main characteristics of the catalytic results.

In the quasi-steady-state regime, remarkable differences in activity and selectivity were obtained with both catalysts. For a more explicit comparison the results are illustrated in Fig. 1 where the activities and the CROTOL yields are compared for both ex-nitrate and ex-chloride catalysts in the first catalytic run and the CROTOL selectivities obtained on both catalysts are compared in the same range of conversions (4–10%), which corresponds to the results reported in the underlined columns of the Tables 1 and 2.

The ex-chloride catalysts showed the highest activities whatever the reduction temperature. For both catalysts the increase in the reduction temperature from 473 to 673 K did not affect significantly the activity, while after reduction at 773 K, the activity decrease was remarkable as clearly illustrated in Fig. 1.

In the stable regime of the ex-nitrate catalysts (Table 1), 29–25% CROTOL selectivity was obtained after 473–573 K reduction; this selectivity increased up to 47% after 673 K reduction and, after 773 K reduction, it decreased in favor of butanal selectivity. These values are compared at the same conversion, about 5%. In fact, after 773 K reduction temperature, the activity of the catalyst was so low that 5% conversion was obtained in the first 10 min of the time on stream. Under these conditions, to get reliable selectivity values in the steady-state regime we increased the reaction temperature knowing that this parameter, in the 313–393 K domain, does not influence significantly the selectivity as will be discussed further. After 773 K reduction temperature the selectivity values were always lower than those found on the catalyst reduced at 673 K. In contrast, on the ex-chloride catalyst (Table 2), in the first catalytic run while the ob-

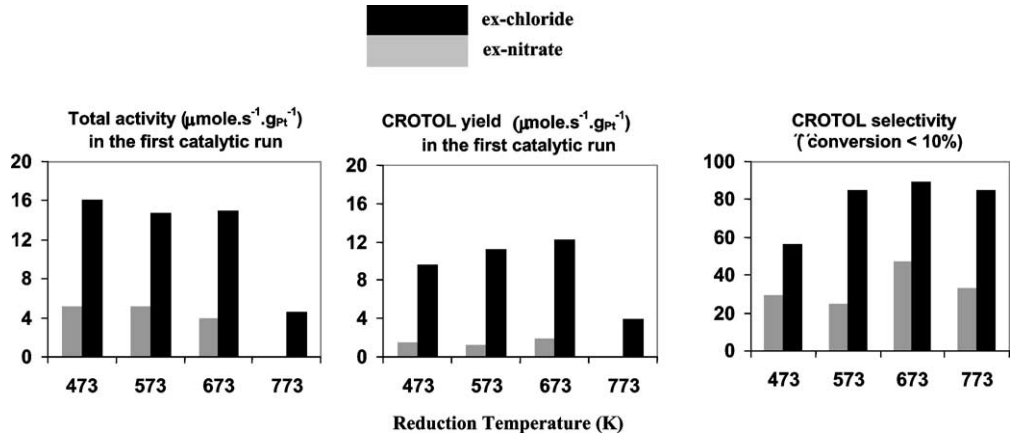

Fig. 1. Crotonaldehyde hydrogenation at 353 K in steady-state regime ($P_{\text{crotonaldehyde}} = 8$ Torr, $P_{H_2} = 752$ Torr).

tained conversions were usually higher than on the ex-nitrate catalyst, a high CROTOL selectivity (60%) was obtained at 473 K reduction and it increased to 76, 81, and 85% after 573, 673, and 773 K reduction, respectively.

To test the reproducibility of the experiments and/or the deactivation, a series of experiments was performed successively, with reduction treatment in-between on the ex-chloride catalyst (Table 2). Whatever the reduction temperature a weak decrease in activity was observed. However, concerning the selectivities, while the values were found independent of the number of cycles after reduction at 473 and 573 K, after reduction at 673 K the selectivities increased to 90% in the fourth catalytic run (with 7% conversion).

The CROTOL yield was higher on the ex-chloride catalysts compared to the ex-nitrate whatever the reduction temperature and the C=O/C=C hydrogenation ratio was lower than 1 on the ex-nitrate catalysts while it reached 6, and even 10 after 4 cycles, on the ex-chloride catalysts.

At 673 K reduction treatment, the experiments were repeated with a lower partial pressure of crotonadehyde (1.5 Torr) in order to increase the contact time of the reactant and then the conversion: the same high selectivity of crotyl alcohol was obtained (89%) in a larger range of conversion (9–23%). Another series of experiments was also performed by varying the reaction temperature in order to gain some information on the activation energy. The results are shown in Table 3, for the ex-chloride catalyst reduced at 673 K. As expected, the increase in the reaction temperature led to an increase in the reaction rate. The activation energies, calculated in the stable regime, in the 313–393 K reaction temperature range, are nearly similar for the C=O and C=C hydrogenation reactions, 20–27 kJ mol^{-1}. This low value is similar to that reported by Vannice and Sen [5] obtained on Pt/TiO_2 in the same reaction. On the other hand, the high stability and activity of this catalyst and the fact that the selectivities are independent of the reaction temperature (in the 353–393 K range) permit us to repeat the experiments changing the experimental parameters (catalyst weight, flow rate, reaction temperature) and then to draw a curve representing the selectivity as a function of the conversion, data

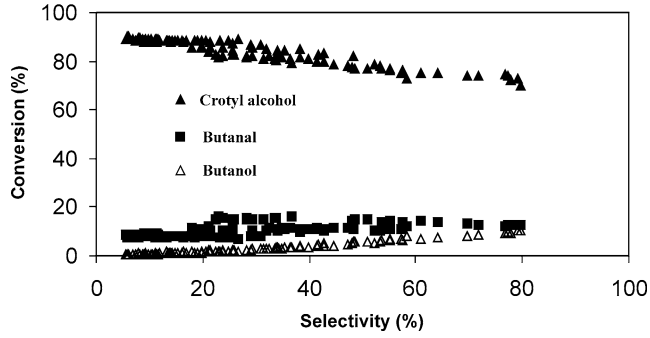

Fig. 2. Crotonaldehyde hydrogenation on 1% Pt/ZnO catalyst, ex-chloride: selectivity as a function of conversion (data taken from several experiments in the quasi-steady-state regime).

Table 4
Atomic absorption spectroscopy results

Treatment		ZnO	1% Pt/ZnO, ex-chloride	1% Pt/ZnO, ex-nitrate
	Pt (wt%)		1.1	0.75
Calc. 623 K	Cl (wt)	$\leqslant 200$ ppm	1.3	$\leqslant 200$ ppm
Reduced 573 K	Pt (wt%)		1.2	
	Cl (wt%)		1.2	
Reduced 673 K	Cl (wt%)		0.5	
Reduced 773 K	Cl (wt%)		< 0.2	

taken in the steady-state regime (Fig. 2). It is remarkable that the CROTOL selectivity *remains higher than* 70 *up to* 80% *conversion*.

Various techniques were used to characterize the ex-nitrate and ex-chloride catalysts in order to get information on their structure and try to determine which are the main factors which could explain the large differences observed in the catalytic behaviors of these two types of catalyst.

Atomic absorption spectroscopy results (Table 4) indicate that after calcination or reduction treatment at a temperature lower that 773 K, chlorine remained on ex-chloride catalysts, after 773 K, the chlorine quantity decreased, but this quantity was higher in comparison with that obtained on

Table 5
BET results

Treatment	ZnO	1% Pt/ZnO, ex-chloride		1% Pt/ZnO, ex-nitrate	
	BET (m^2/g)	BET (m^2/g)	V_p (cm^3/g)	BET (m^2/g)	V_p (cm^3/g)
Calc. 623 K	24.6	24.9	0.26	24.4	
Reduced 473 K		13.9	0.12	22.3	0.12
Reduced 673 K		9.0		18.3	
Reduced 773 K		4.0		9.6	0.03

Table 6
TEM analyses: Particle sizes (d's in nm) for ex-nitrate and ex-chloride 1% Pt/ZnO catalysts, reduced at different temperatures

Catalysts	Ex-chloride	Ex-nitrate
Reduced 473 K	1–2 nm	1–2
Reduced 673 K	4.3	3
Reduced 773 K	12.5	5

ex-nitrate catalysts. On ex-nitrate catalysts the presence of chlorine comes from ZnO itself.

BET results (Table 5) show that, after calcination treatment, the ZnO surface area has not changed after platinum salt impregnation, for both catalysts. After 473 K reduction treatment, the surface area decreased significantly on the ex-chloride catalysts, but no change was observed on the ex-nitrate catalysts.

In the TEM images, the metal particles appeared as homogeneously dispersed on the support, for both catalysts. The sizes of particles, measured after reduction at 473, 673, and 773 K are reported in Table 6. It is worthwhile to note that the particle sizes, for both catalysts, were situated in the same range. To be precise we note that, after reduction at 473 K, the contrast between metal and support was not good enough to measure a large number of particles, but the visible particles were between 1 and 2 nm. The particle sizes increased more significantly on the ex-chloride catalyst compared to the ex-nitrate, particularly after reduction at 773 K.

The XRD results are reported in Fig. 3 for the ex-chloride catalysts after reduction treatment at temperature $\geqslant$ 673 K: the PtZn diffraction lines only were observed. At lower reduction temperature no diffraction lines could be discerned. For the ex-nitrate catalysts, whatever the reduction temperature, $\leqslant$ 773 K, no diffraction line was discerned, because of the too small particle sizes in accordance with the TEM analyses.

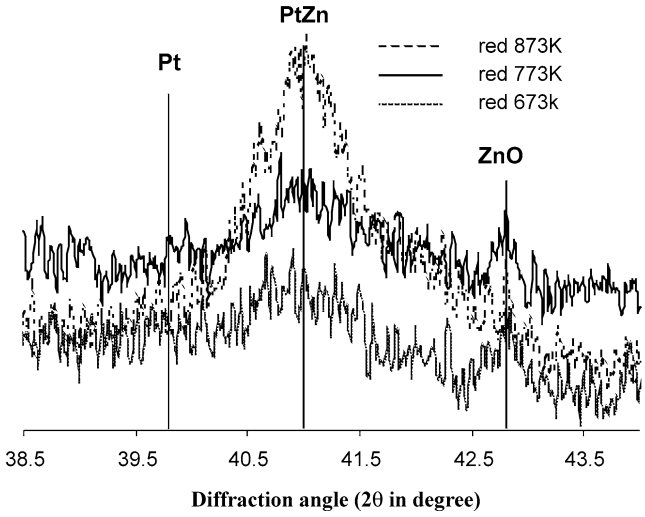

Fig. 3. XRD analysis on 1% Pt/ZnO, ex-chloride catalyst.

The XPS measurements are shown in Table 7 which show the Pt ($4f_{7/2}$) BE, the Lorentzian half-width (γ), and the value of the atomic ratios of the different elements obtained after the fitting procedure. For the ex-chloride catalyst and after reduction, the Pt($4f_{7/2}$) BE value, 70.9 ± 0.1 eV, is characteristic of platinum in a reduced state. In the calcined sample the Pt($4f_{7/2}$) BE (71.9 eV) is characteristic of PtO compound, according to Hecq et al. [18] and Bancroft et al. [19]. We also remark that γ decreased from 0.36 to 0.3 and to 0.11 when the reduction temperature increased from 473 to 573 or 673 K and then to 773 K; this corresponds

Table 7
XPS results of 1% Pt/ZnO catalysts

	Treatment	Pt		Pt/Zn ∗ 100	Cl/Zn
		BE($Pt_4f_{7/2}$) (eV)	γ (eV)		
1% Pt/ZnO, ex-chloride	Calc. 623 K	71.9	0.99	1.9	0.15
	Reduced 473 K	71.0	0.35	1.9	0.16
	Reduced 573 K	70.9	0.31	1.7	0.18
	Reduced 673 K	70.8	0.31	1.7	0.17
	Reduced 773 K	70.7	0.11	4.0	0.10
1% Pt/ZnO, ex-nitrate	Calc. 623 K	71.3	1.14	0.9	0.10
	Reduced 473 K	71.0	0.67	0.9	0.08
	Reduced 573 K	71.0	0.78	1.0	0.06
	Reduced 673 K	70.8	0.50	0.9	0.08
	Reduced 773 K	70.8	0.38	1.5	0.05

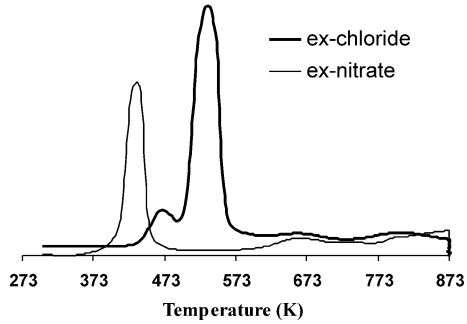

Fig. 4. TPR profiles on 1% Pt/ZnO catalysts precalcined at 673 K.

to a decrease in the lifetime of the core hole as usually observed when going from monometallic to alloy compound. On the other hand, in the calcined ex-nitrate catalysts, the Pt($4f_{7/2}$) line was fitted with one contribution at 71.3 eV and a large γ (1.14), but that was less realistic than fitting with two components corresponding to reduced and oxidized species, respectively, revealing the presence of reduced Pt particles surrounded by a platinum oxide layer. In the ex-nitrate catalysts, after reduction treatment, platinum was actually reduced (BE $= 70.9 \pm 0.1$ eV) and no change was observed when increasing the reduction temperature to 773 K. It is important to note that γ values were higher in the ex-nitrate than in the ex-chloride catalysts and they still decreased from 0.7 to 0.5 and to 0.37 when the reduction temperature increased from 473 to 673 and to 773 K which is interpreted as the presence of a Pt–Zn alloy after reduction at 673 K and higher reduction temperatures. The Pt/Zn atomic ratios are higher in the ex-chloride catalysts compared to the ex-nitrate, whatever the reduction temperature and this ratio increases at high reduction temperatures and more significantly on the ex-chloride than on the ex-nitrate. The latter observation should be correlated to the evolution of the surface area of the support which decreased when the reduction temperature increased and much more significantly on the ex-chloride than on the ex-nitrate (see Table 5). Higher ratios observed on the ex-chloride catalysts could be alternatively explained if the particle sizes were smaller but the inverse trend was revealed from the XRD and TEM analysis. Therefore, the high Pt/Zn ratios indicate that the metallic particles are localized at the outer surface of the support in the ex-chloride catalyst while they should be inside the pores in the ex-nitrate catalysts. As could be expected the Cl/Zn atomic ratios were higher on the ex-chloride (2 or 3 times) than on the ex-nitrate catalysts where it is not zero due to the presence of Cl initially contained in the support. However, on the ex-chloride catalyst, this ratio decreased from 0.16 to 0.10 when the reduction temperature increased from 473 to 773 K. It means that a reduction temperature as high as 773 K is necessary to begin to remove some of the chlorine from the catalyst surface. In the bulk (Table 4), the chlorine amount decreased after 673 K reduction temperature.

The TPR profiles are reported in Fig. 4. The ex-nitrate catalyst presented a reduction maximum at 433 K, with a H_2/Pt ratio equal to 1.5, while the ex-chloride one presented a small peak followed by a large peak of H_2 consumption appearing at higher temperatures, 473 and 533 K, respectively. On Pt/Al_2O_3 prepared from chlorinated precursor, Marceau et al. [20] indicated the presence of oxy-chlorinated Pt species, which were reduced at 563 K, while Hwang and Yeh [21] reported that dispersed PtO_xCl_y species were reduced at a higher reduction temperature (623 K). The TPR profiles of the ex-chloride catalysts obtained on the 1 and 5% Pt catalysts [13] are similar. However, while the 5% Pt/ZnO XPS analysis performed on the calcined samples confirmed the presence of oxychloride platinum species, on the 1% Pt/ZnO catalyst, there is no indication of chlorinated platinum species by XPS. That could be due to the much larger dispersion of the oxychloride species which would not be stable under the X-ray beam and would decompose to form PtO species.

The high consumption of H_2 (H_2/Pt $= 3.3$) was in accordance with that already observed on 5% Pt/ZnO [13] or in Pt/Al_2O_3 [22,23] which was interpreted by the authors, from EXAFS characterization, by the following equation:

$$\left[\mathrm{Pt(OH)_4(Cl)_2}\right]^{2-} + 3\mathrm{H_2} \rightarrow \mathrm{Pt^0} + 4\mathrm{H_2O} + 2\mathrm{HCl} + 2e^-.$$

In the ex-nitrate catalysts, the TPR profile is well explained by assuming the reduction of small PtO_2 particles containing a core made of metal platinum since H_2/Pt was smaller than the stoichiometry governed by the equation $PtO_2 + 2H_2 \rightarrow Pt + 2H_2O$.

After 573 K, reduction of ZnO support is visible on both spectra.

3.2. CO adsorption study by FTIR

CO adsorption on metal involves two types of bonds, σ and π bonds. The π bond results from a back-bonding of "d" electrons from the metal to π^* antibonding orbital of CO which consequently decreases the force constant of the CO bond and lowers the CO vibration frequency in comparison with gaseous CO [24]. Moreover, it must be noted that the frequency, ν(CO), of the species Pt–CO increases when the coverage of the metallic surface increases, due to the dipole–dipole coupling interaction [25]. Fig. 5 shows the spectra of the CO adsorption band, in the 2200–2000 cm^{-1} region, recorded at room temperature on the ex-chloride and ex-nitrate catalysts precalcined at 673 K ex situ followed by in situ evacuation and reduction at 473 K. For the ex-chloride catalyst, when the first dose of CO was adsorbed on the catalyst, the ν(CO) was situated at 2053 cm^{-1} and this frequency does not change significantly when additional doses were adsorbed while, for the ex-nitrate catalyst, it appeared at lower frequency, 2016 cm^{-1}, after the first dose had been introduced to increase up to 2030 cm^{-1} at higher coverage. Therefore the ex-chloride catalyst shows definitely a higher ν(CO) vibration frequency than the ex-nitrate catalyst which indicates a difference in the back donation of the d electrons

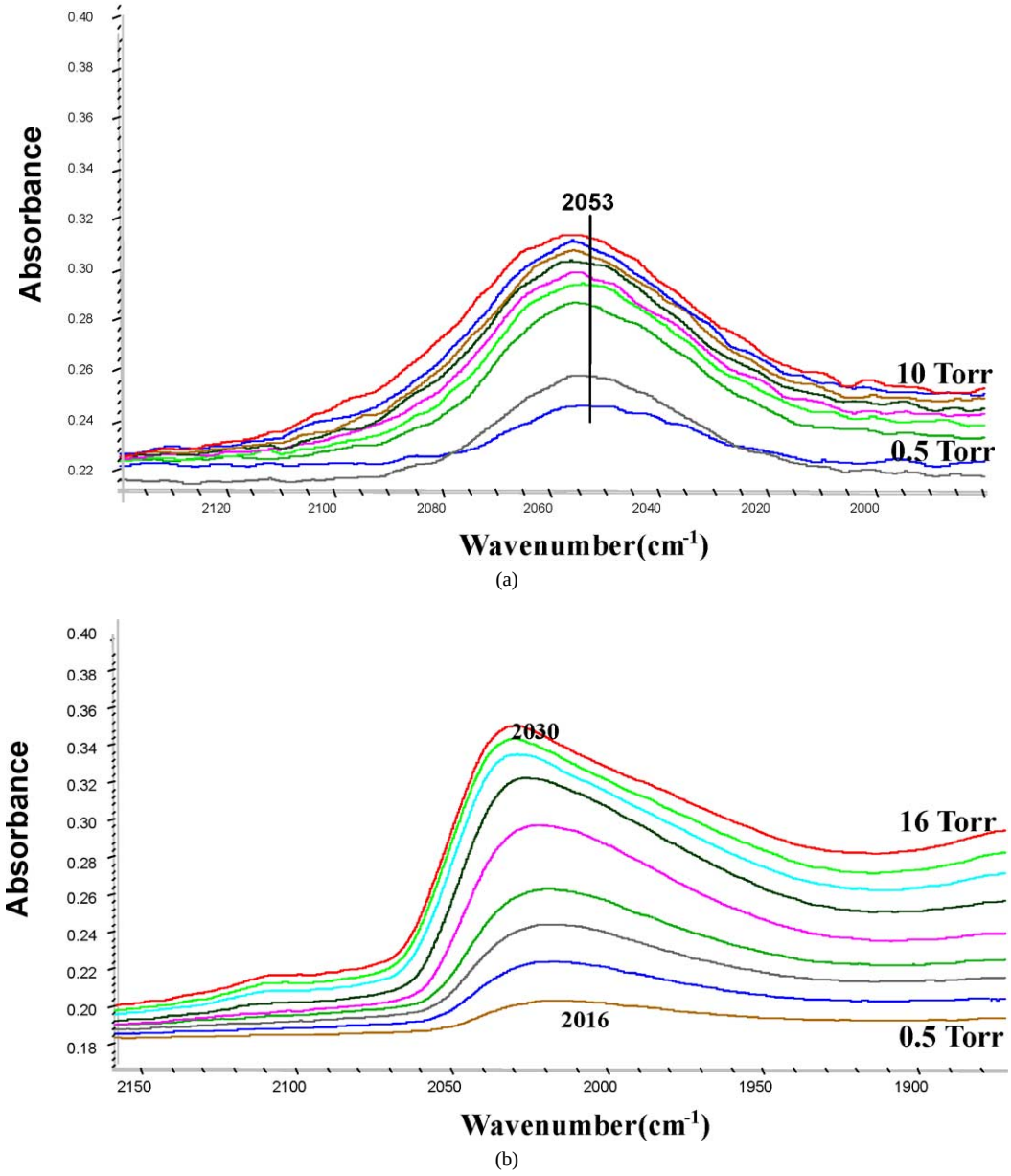

Fig. 5. FTIR spectra of CO adsorbed on 1% Pt/ZnO, after evacuation at 673 K and reduction at 473 K on (a) ex-chloride catalyst, (b) on ex-nitrate catalyst, as a function of addition of small quantities of CO (from 0.5 to 10–16 Torr).

of platinum. Platinum atoms would be more electron deficient on the ex-chloride catalyst compared to the ex-nitrate catalyst. Keeping in mind that the particle sizes of Pt after 473 K reduction are similar on both catalysts, the variation of the Pt electronic character between both catalysts originates from elsewhere, either alloy or support effects as will be discussed later. The broadness of the CO band in interaction with Pt particles and the shift of the CO wavenumbers from 2016 to 2030 cm^{-1} when coverage increases on the ex-nitrate catalyst suggest a heterogeneity of the adsorption sites likely adsorption on terrace, step, or corner sites. But, static and dynamic coupling can also explain this wavenumber shift. The question which arises is why the wavenumber does not vary with the coverage in the case of the ex-chloride catalyst. Two reasons could be suggested:

(i) the higher acidity of the support leading to a lower back-donation from Pt toward CO could induce a weaker sensitivity of the ν(CO) value to the CO coverage,
(ii) the presence of PtZn alloy in the ex-chloride, formed at 473 K reduction temperature, involves a dilution of the Pt atoms which leads to an insensitivity to the CO coverage.

Adsorption experiments performed after higher reduction temperature, 673 K, led to a complete loss in IR trans-

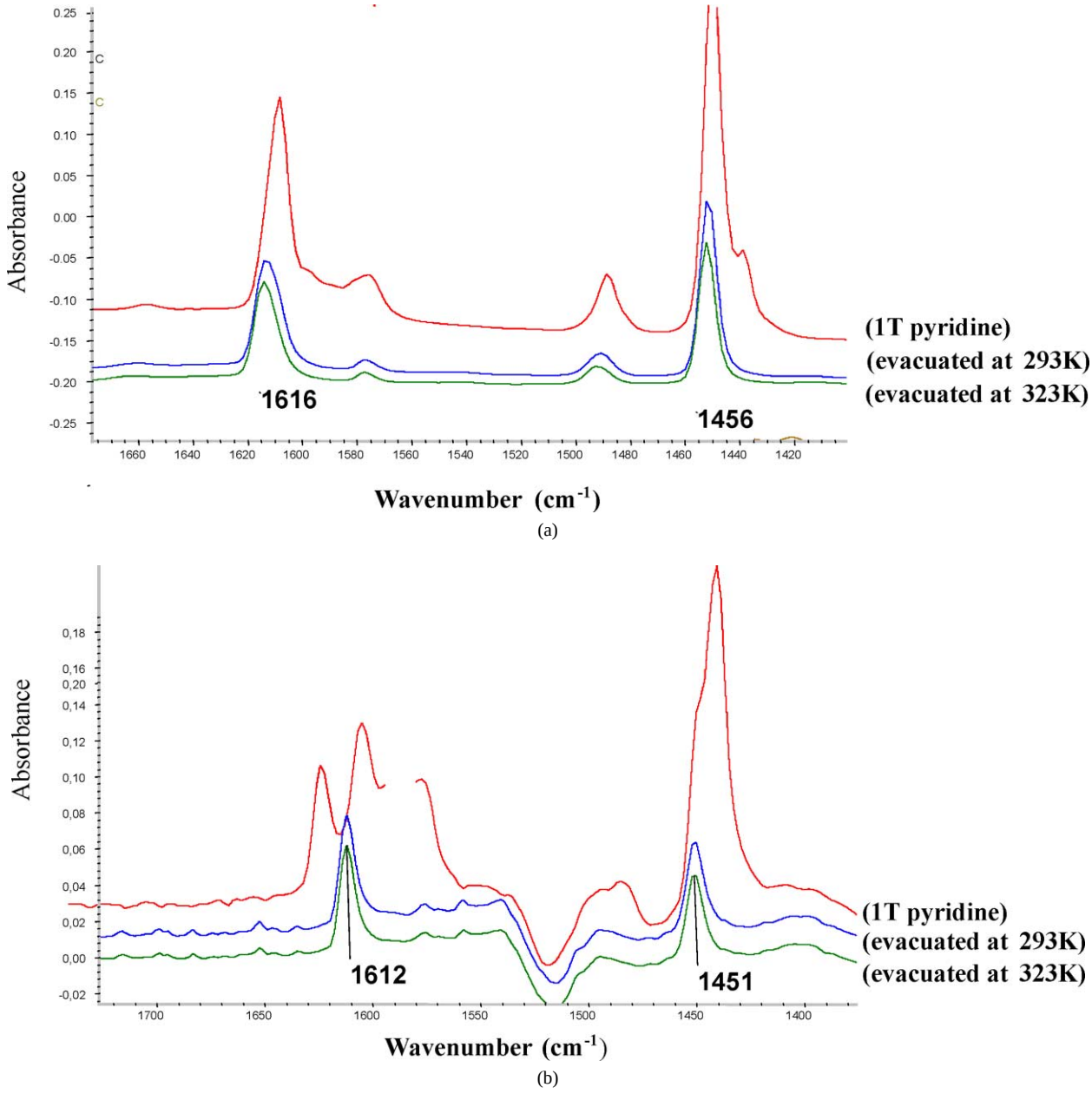

Fig. 6. FTIR spectra of pyridine adsorbed on (a) ex-chloride catalyst, and (b) ex-nitrate catalyst.

parency. This is due to the too high reduction of ZnO as it is well confirmed by a reduction peak appearing at this temperature on the TPR spectra. After H_2 chemisorption on the Pt/ZnO system, the H atoms spill over into the ZnO and offer free electrons which interact with the IR radiation [26,27] and then there is no more energy transmission.

3.3. Pyridine adsorption by FTIR

Fig. 6 shows the IR spectra obtained after pyridine adsorption at room temperature and evacuation at 293 and 323 K, on the ex-chloride (a) and ex-nitrate (b) catalysts prereduced at 373 and 473 K, respectively. For the two catalysts, there is no band around 1540–1550 cm^{-1}, which indicates that there are no Brønsted acid sites on Pt-supported ZnO systems [28]. However, in the ex-nitrate catalyst, two bands were observed, at 1612 and 1451 cm^{-1}. These bands correspond to the ν_{8a} and ν_{19b} vibration modes, respectively. These vibrations are characteristic of the coordinately bonded pyridine. The ν_{8a} vibration is sensitive to the mode of adsorption and informs on the nature and on the strength of the Lewis acidity, while the ν_{19b} vibration is characteristic of the number of sites existing on the surface [29]. In addition to the two main bands, additional bands, at 1574, 1600, and at 1625 cm^{-1}, were present, after pyridine adsorption, but disappeared after evacuation treatment at 293 or at 323 K. These bands correspond to the hydrogen-bonded pyridine, indicating the existence of OH groups on the cata-

lyst surface. Interestingly, on the ex-chloride catalyst, these bands, characteristic of the existence of OH groups on the surface, are hardly visible compared to the ex-nitrate catalyst; in fact, OH^- are replaced by Cl^- on the ex-chloride catalysts. Moreover, the ν_{8a} and ν_{19b} vibrations shifted toward higher frequencies. These vibrations were situated at 1616 and 1456 cm^{-1}, respectively. This reveals a stronger Lewis acidity in the ex-chloride in comparison with the ex-nitrate catalysts. Moreover, a higher intensity of the ν_{19b} bond was obtained. That suggests a higher number of Lewis acid sites.

4. Discussion

From the catalytic results, ex-chloride and ex-nitrate 1% Pt/ZnO catalysts exhibit different behavior in crotonadehyde hydrogenation with much better performances for the ex-chloride catalysts. These results are in line with those obtained on the 5% Pt/ZnO catalysts [13]. However, the ex-chloride 1% Pt/ZnO catalyst is superior to its corresponding 5% Pt/ZnO since it was more active, more stable, and still more selective in crotyl alcohol formation. We shall first discuss the alloy and chlorine promoter effects evidenced by the correlation between activity and structure and then we shall attempt a description at the molecular scale of the catalytic site involved in the crotonaldehyde hydrogenation on Pt/ZnO catalyst.

4.1. Alloy promoter effect

At 353 K reaction temperature the best result of crotyl alcohol selectivity obtained on the ex-nitrate catalysts was 47% after reduction at 673 K. A higher reduction temperature reduction (773 K) led to a loss in activity at 353 K, and at a higher reaction temperature (413 K), in the stable regime, a decrease in the selectivity to 34% was observed. In comparison, for the ex-chloride catalyst, after 473 K reduction, the crotyl alcohol selectivity reached 70%, which increased to 85% after higher reduction temperatures (573–773 K). It appears then that an increase in reduction temperature from 573 to 773 K on the ex-chloride catalysts has no effect on the selectivity while, on the ex-nitrate catalysts an improvement in the crotyl alcohol selectivity was induced by the increase of the reduction temperature. On the other hand, the formation of a PtZn alloy after reduction at 673 K or higher was observed by XRD on the ex-chloride catalysts. On the ex-nitrate catalyst, the particles sizes were too small to give any information by XRD analyses but the narrowing of the Pt 4f lines in XPS observed when the reduction temperature increased from 473 to 673 K revealed the transformation of Pt to PtZn alloy. Moreover, on the 5% Pt/ZnO system [13], XRD and XPS combined results indicated clearly that PtZn alloy was formed only after 573 K reduction on the ex-nitrate catalyst while, on the ex-chloride, it was already formed at 473 K reduction. A similar behavior for the 1% Pt/ZnO system could be assumed as revealed by the narrowness of the Pt 4f lines of the ex-chloride catalyst observed even at low reduction temperature (473 K). Therefore, on the ex-chloride catalyst, the Pt particles would be present as a mixture of pure Pt and alloyed Pt–Zn particles at 473 K and form pure Pt–Zn alloy from 573 K reduction, while the transformation from metal to alloy occurs only from 573 K on the ex-nitrate catalysts. From these results, we propose that PtZn alloy formation was responsible for the selectivity increase which occurred in parallel with the increase in the reduction temperature for both catalysts. However, beside this beneficial alloy effect on the selectivity, it is clear that there is an additional promoter effect due to the presence of chlorine.

4.2. Chlorine promoter effect

It is remarkable that chlorine has a beneficial effect on both selectivity and activity in the Pt/ZnO system. The total activities on the ex-chloride catalyst are 3 times higher than obtained on the ex-nitrate catalyst and the crotyl alcohol yields are 6–9 times higher, whatever the reduction temperature from 473 to 673 K (Table 1, Fig. 1). It is clear that the difference does not originate from the metallic particle sizes which are in the same range on both catalysts. On the other hand, nothing can be deduced from the activation energy which is similar for both C=C and C=O bond hydrogenation and similar to the published results, independently of the catalysts. In contrast, the results coming from the pyridine adsorption in FTIR show interesting differences in the Lewis acidity of both catalysts. The Lewis acidity was stronger and the sites more numerous on the ex-chloride catalyst compared to the ex-nitrate, after reduction at 473 K. Therefore chlorine atoms coming from the decomposition of the metallic precursor influence the structure of the support (decrease of the surface area, Table 5) and the acidity of the support. This acidity could influence the electronic properties of the metal particle since the vibration frequency of CO (FTIR) adsorbed on platinum was shifted at a higher energy on the ex-chloride catalyst.

4.3. Adsorption mode of crotonaldehyde on Pt/ZnO

However, after 473 K reduction, the presence of alloy in the ex-chloride catalyst while the ex-nitrate catalyst contains only pure metal could also explain the blue shift of the IR frequency observed from the ex-nitrate to the ex-chloride. Rodriguez and Kuhn [30] reported photoemission and CO TPD studies performed on a PtZn surface alloy obtained by heating a Pt (111) monocrystal covered by zinc. They concluded that the formation of PtZn bonds produces a large depletion in the density of Pt 5d electrons around the Fermi level, with a shift in the centroid of the Pt 5d band. This is accompanied by an important redistribution of charges, in which Pt loses 5d electrons and gains (6s, 6p)

electrons. The authors show also that the electronic perturbations induced by zinc on Pt reduce its CO-chemisorption ability by weakening the strength of the Pt(5d)–CO($2\pi^*$) bonding interactions. If one applies these conclusions to our catalysts composed of PtZn nanoparticles, the electronic perturbations, implying a decrease in 5d electron population of platinum, will weaken the strength of the Pt–(C=C) bonding and then the hydrogenation into butanal. Moreover, it is probable that the Lewis acidity, due to the presence of chlorine atom and oxygen vacancies, creates an electrostatic field which decreases further the d population at the Fermi level. This positively polarized platinum surface could change the adsorption mode of the crotonaldehyde by binding the electron pair of the terminal oxygen with the holes in the d band. The adsorption mode by the terminal oxygen would be the precursor state of the hydrogenation reaction of the crotonaldehyde which produces unsaturated alcohol and, in contrast, the olefinic bond would be weakly adsorbed and the production of butanal severely reduced.

An alternative explanation would be to attribute the non-adsorption of the olefinic bond of crotonaldehyde to the specific electronic properties of Pt in PtZn alloy as described previously and crotonaldehyde would adsorb by binding the C=O moiety on the Lewis acidity sites of the ZnO_xCl_y entities localized on the support near the PtZn particles. However, crotonaldehyde hydrogenation performed on exchloride Pd/ZnO catalysts [31] led to 100% butanal selectivity whatever the activity of the catalyst and especially in the same range of activity as Pt/ZnO. It means that the support around the metallic Pd or PdZn particles which has certainly gained the same Lewis acidity properties due to the presence of chlorine and hydrogen treatment is not active for the hydrogenation of the carbonyl bond. Therefore we prefer to attribute the exceptional ability of Pt/ZnO catalysts to hydrogenate selectively the C=O bond in crotonaldehyde to specific electronic properties of platinum gained from both phenomena, PtZn alloy and Lewis acidity of the support which would lead to an electrodeficient character of the metallic surface.

The 1% Pt/ZnO catalysts were found more efficient than the corresponding 5% Pt/ZnO catalysts due to the lower amount of chlorine. In fact, a too large amount of chlorine at the catalyst surface leads to a detrimental additional reaction, transforming crotyl alcohol into crotylchloride and then decreasing the crotyl alcohol selectivity [13]. On the other hand the lower dispersion of the metallic phase in the 5% Pt/ZnO catalyst leads to a less active catalyst.

In conclusion it should be underlined that, by the very simple impregnation method, using chloroplatinic acid deposited on a commercial ZnO support, followed by air-calcination and H_2-reduction treatments at 673 K, 1% Pt/ZnO catalysts were prepared and found able to convert crotonaldehyde into crotyl alcohol with 90–80% selectivity up to 60% conversion in the 313–393 K reaction temperature range. To our knowledge, these performances are so far the best ones found on Pt-based catalysts for selective hydrogenation of crotonaldehyde into unsaturated alcohol. However, Pt/ZnO catalysts will definitely be a emergent catalytic material if these good properties found for a model reaction performed in the gas phase remain when tested in the liquid phase, under industrial conditions.

References

[1] P.N. Rylander, Catalytic Hydrogenation over Platinum Metal, Academic Press, New York, 1967.
[2] P. Gallezot, D. Richard, Catal. Rev.-Sci. Eng. 40 (1998) 81.
[3] V. Ponec, Appl. Catal. A 149 (1997) 27.
[4] S. Galvagno, G. Capannelli, G. Neri, A. Damato, R. Pietropaolo, J. Mol. Catal. 35 (1986) 365.
[5] M. English, V.S. Ranade, J.A. Lercher, J. Mol. Catal. 121 (1997) 69.
[6] M.A. Vannice, B. Sen, J. Catal. 115 (1989) 65.
[7] B. Sen, M.A. Vannice, J. Catal. 113 (1988) 52.
[8] A. Sepulveda-Escribano, F. Coloma, F. Rodriguez-Reinoso, J. Catal. 178 (1998) 649.
[9] A. Sepulveda-Escribano, J. Silvestre-Albero, F. Coloma, F. Rodriguez-Reinoso, Stud. Surf. Sci. Catal. 130 (2000) 1013.
[10] M. Abid, R. Touroude, Catal. Lett. 69 (2000) 139.
[11] M. Abid, G. Ehret, R. Touroude, Appl. Catal. 217 (2001) 219.
[12] K. Liberkova, R. Touroude, J. Mol. Catal. A 180 (2002) 221.
[13] M. Consonni, D. Jokic, D.Yu. Murzin, R. Touroude, J. Catal. 188 (1999) 165.
[14] A. Boffa, C. Lin, A.T. Bell, G.A. Somorjai, Catal. Lett. 27 (1994) 243.
[15] M. Englisch, A. Jentys, J.A. Lercher, J. Catal. 166 (1997) 25.
[16] J.L. Margitfalvi, A. Tompos, I. Kolosova, J. Valyon, J. Catal. 174 (1998) 246.
[17] A. Dandekar, M.A. Albert, J. Catal. 183 (1999) 344.
[18] M. Hecq, A. Hecq, J.P. Delrue, T. Robert, J. Less-Common Met. 64 (1979) P25.
[19] G.M. Bancroft, I. Adams, L.L. Coatsworth, C.D. Bennewitz, J.D. Brown, W.D. Westwood, Anal. Chem. 47 (1975) 586.
[20] E. Marceau, M. Che, J. Saint-Just, J.M. Tatibouët, Catal. Today 29 (1996) 415.
[21] C. Hwang, C. Yeh, J. Mol. Catal. 112 (1996) 295.
[22] F. Le Normand, A. Borgna, T.F. Garetto, R. Apesteguia, B. Moraweck, J. Phys. Chem. 100 (1996) 9068.
[23] A. Borgna, T.F. Garetto, C.R. Apesteguia, F. Le Normand, B. Moraweck, J. Catal. 186 (1999) 433.
[24] M. Primet, J.M. Basset, M.V. Mathieu, M. Prettre, J. Catal. 29 (1973) 213.
[25] R.P. Eischens, W.A. Pliskin, Adv. Catal. Relat. Subj. 10 (1958).
[26] F. Boccuzzi, A. Chiorino, G. Chiotti, F. Pinna, G. Strukul, R. Tessari, J. Catal. 126 (1990) 381.
[27] W. Li, Y. Chen, C. Yu, X. Wang, Z. Hong, Z. Wei, in: Proc. 8th Int. Congress on Catalysis, Vol. 5, Berlin, 1984, p. 205.
[28] E.P. Parry, J. Catal. 2 (1963) 371.
[29] G. Berhault, M. Lacroix, M. Breysse, F. Maugé, J.-C. Lavalley, H. Nie, L. Qu, J. Catal. 178 (1998) 555.
[30] J.A. Rodriguez, M. Kuhn, J. Chem. Phys. 102 (1995) 4279.
[31] F. Ammari, Thesis, Strasbourg, 2002.